Supplementary material

Combination of Super-Resolution Fluorescence and Magnetic Resonance Imaging by a Mn(II) compound

Xiaohe Tian[abc*‡], Lufei Xiao[bd‡], Yu Shen[b], Lei Luo[e], Guilong Zhang[f], Qiong Zhang[b], Dandan Li[bc], Jieying Wu[b], Zhengyan Wu[f*], , Zhongping Zhang[bg] , Yupeng Tian[b]

[a]*School of Life Science, Anhui University, Hefei 230039, P. R. China, xiaohe.t@ahu.edu.cn*

[b]*Department of Chemistry, Key Laboratory of Functional Inorganic Material Chemistry of Anhui Province, Anhui University, Hefei 230039, P. R. China*

[c]*Institute of Physical Science and Information Technology, Anhui University, Hefei 230039, P. R. China*

[d]*Department of Food and Environmental engineering, Chuzhou Vocational and Technical college, Chuzhou 239000, P. R. China*

[e]*College of Pharmaceutical Sciences, Southwest University, Chongqing 400716, China*

[f]*Key Laboratory of High Magnetic Field and Ion Beam Physical Biology, Hefei Institutes of Physical Science, Chinese Academy of Sciences, Hefei 230031, P.R. China*

[g] *CAS Center for Excellence in Nanoscience, Institute of Intelligent Machines, Chinese Academy of Sciences, Hefei 230000, P. R.China*

* Correspondence: E-mail: xiaohe.t@ahu.edu.cn； zywu@ipp.ac.cn

‡ These authors contributed equally to this work.

Contents

Synthesis of L^1 and L^2

L^1 and L^2 were prepared according to the reported works.[1, 2]

Preparation and characterization of MnFM1 and MnFM2

MnFM1. $\mathbf{L^1}$ (0.202 g, 0.400 mmol) and $Mn(OAc)_2{\cdot}4H_2O$ (0.049 g, 0.200 mmol) were dissolved in EtOH (20 mL). The mixture was refluxed for 3 h and then 10 mL EtOH containing KPF_6 (0.074 g, 0.400 mmol) was added in. The mixture continued to reflux for 1 h, and part of the solvent was removed, then the solid appeared, filtered while hot. The product was washed with H_2O and EtOH for 3 times, and dried in vacuo. Yield: 0.206 g (75.90 %). ^{1}H NMR (400 MHz, d_6-DMSO, ppm): δ 8.72 (d, *J*=31.1 Hz, 12H), 8.04 (s, 4H), 7.86 (s, 4H), 7.52 (s, 4H), 7.34 (s, 8H), 7.11 (s, 14H), 5.15 (s, 2H), 4.49 (s, 4H). IR (cm^{-1}): 3421 (m), 3063 (m), 2922 (m), 1587 (vs), 1512 (s), 1475 (s), 1417 (m), 1329 (s), 1288 (m), 1196 (s), 1017 (m), 844 (s), 792 (s), 760 (m), 698 (m), 658 (m), 640 (m), 558 (s), 522 (m). ESI-MS: m/z (100 %), 534.50 (100%). Anal.Calcd for $C_{68}H_{52}F_{12}MnN_8O_2P_2$: C, 60.14; H, 3.86; N, 8.25. Found: C, 60.39; H, 3.88; N, 8.28.

MnFM2. The same procedure as that for **MnFM1** was used except that $\mathbf{L^1}$ was replaced by $\mathbf{L^2}$ (0.214 g, 0.400 mmol). Yield: 0.211 g (74.45%). ^{1}H NMR (400 MHz, d_6-DMSO, ppm): δ 8.72 (d, *J*=30.9 Hz, 12H), 8.03 (s, 4H), 7.85 (s, 4H), 7.52 (s, 4H), 7.32 (s, 8H), 7.09 (s, 13H), 5.15 (s, 4H), 4.49 (s, 8H). IR (cm^{-1}): 3393 (m), 3063 (m), 2922 (m), 2872 (m), 1593 (vs), 1510 (s), 1475 (s), 1417 (m), 1327 (s), 1288 (m), 1197 (s), 1016 (s), 844 (vs), 791 (s), 731 (m), 671 (m), 658 (m), 639 (m), 558 (s), 521 (m). ESI-MS: m/z (100%), 564.33 (100%). Anal.Calcd for $C_{70}H_{56}F_{12}MnN_8O_4P_2$: C, 59.29; H, 3.98; N, 7.90. Found: C, 59.50; H, 4.00; N, 7.93.

Materials, Methods and Instruments

Materials. 5-dimethylthiazol-2-yl-2,5 –diphenyltetrazolium bromide (MTT) were purchased from Sigma. Triphenylamine, 2-acetylpyridine, Phosphorus oxychloride and other chemicals used were received from Sinopharm Chmical Reagent Co., Ltd. Cell fluorescent marker including NucRed, ER tracker were obtained from Thermofisher (USA). Primary MAP2 antibody and its secondary antibody were supplied by Abcam (USA).

General procedure. FT-IR spectra were recorded in the solid (KBr disk) on a NEXUS-870 (Nicolet) spectrophotometer in the 400-4000 cm^{-1}. Elemental analyses (C, H, and N) were performed using a Perkin-Elmer 240 analyzer. The ^{1}H and ^{13}C NMR spectra were collected on a BrukerAvance 400 spcetrometer at 25 °C, and the chemical shifts were reported as parts per million (ppm) from TMS. Coupling constants *J* were given in Hertz. Mass spectra were recorded on a Micromass GCT-MS (ESI source) and BrukerAutoflex III SMartbeam (MALDI-TOF). Room-temperature EPR spectra of complexes powder were obtained using aJEOL JES-FA200 EPR spectrometer (300 K, 9.063 GHz, X-band). Microwave power employed was 1mW. Modulation frequency and modulation amplitude were 100 kHz and 0.35mT, respectively. g =0.07145×γ(MHz)/H(mT), γ: microwave frequency; H: resonance field.

X-ray crystallography and structure solution. X-ray diffraction data of single crystals were collected on a Siemens Smart 1000 CCD diffractometer, and the determination of unit cell parameters and data collections were performed with Mo-Kα radiation (λ=0.71073Å). Unit cell dimensions were collected with least-squares refinements and all structures were solved by direct methods using SHELXS-97. The other non-hydrogen atoms were located in successive difference Fourier syntheses. The final refinement was performed by full-matrix least-squares methods with anisotropic thermal parameters for non-hydrogen atoms on F^2. The hydrogen atoms were added theoretically and riding on the concerned atoms.

Optical measurements. The linear absorption spectra were recorded on a UV-3100 spectrophotometer. The single-photon excited fluorescence (SPEF) spectra were obtained using a F-2500 fluorescence spectrophotometer. The quartz cuvettes used are of 1 cm path length. The fluorescence quantum yields (Φ) were determined against the quinine sulfate (in 1 N H_2SO_4, Φ=0.54) standard. Quantum yields were corrected as follows:

$$\Phi_s = \Phi_r \left(\frac{A_r \eta_s^2 D_s}{A_s \eta_r^2 D_r} \right)$$

Where the s and r indices designate the sample and reference samples, respectively, A is the absorbance at λ_{exc}, η is the average refractive index of the appropriate solution, and D is the integrated area under the corrected emission spectrum.

Optimizations were carried out with B3LYP functional without any symmetry restraint, and the time-dependent density functional (TD-DFT) calculations were performed on the optimized structure with B3LYP functional. All calculations, including optimizations and TD-DFT, were performed with the G03 software. Geometry optimization of the singlet ground state and the TD-DFT calculation of the lowest 25 singlet-singlet excitation energies were calculated with a basis set composed of 6-31 G* for C H N O atoms and the Lanl2dz basis set for Mn atom was downloaded from the EMSL basis set library. An analytical frequency confirms evidence that the calculated species represents a true minimum without imaginary frequencies on the respective potential energy surface. The lowest 25 spin-allowed singlet-singlet transitions, up to energy of about 5 eV, were taken into account in the calculation of the absorption spectra.

For time-resolved fluorescence measurements, the fluorescence signals were collimated and focused onto the entrance slit of a monochromator with the output plane equipped with a photomultiplier tube (HORIBA HuoroMax-4P). The decays were analyzed by 'least-squares'. The quality of the exponential fits was evaluated by the goodness of fit (χ^2).

2PA cross-sections (δ) of the samples were obtained by two-photon excited fluorescence (TPEF) method at femtosecond laser pulse and Ti: sapphire system (680–1080 nm, 80 MHz, 140 fs) as the light source. The sample was dissolved in DMSO at a concentration of 1.0×10^{-3}mol L^{-1}. The TPEF intensity of the reference and the sample were determined at their excitation wavelength. Thus, 2PA cross-section (δ) of samples was determined as follows:

$$\delta = \delta_{ref} \frac{\Phi_{ref}}{\Phi} \frac{c_{ref}}{c} \frac{n_{ref}}{n} \frac{F}{F_{ref}}$$

Where the ref subscripts stand for the reference molecule (here fluorescein was used as reference). δ is the 2PA cross-sectional value, c is the concentration of the solution, n is the refractive index of the solution, F is the TPEF integral intensities of the solution emitted at the exciting wavelength, and Φ is the fluorescence quantum yield.

Cell culture. HepG2 cells (ATCCCRL-2299) and HELF cells were seeded on a T-75 flask, maintained in DMEM medium (Dulbecco's Modified Eagle's Medium-high glucose, D5671-SIGMA) supplemented with 2 mM L-glutamine, 100 IU/mL penicillin, 100 mg/ml streptomycin, and 10 % fetal calf serum (FCS). Cultures were maintained at 37 °C in an atmosphere of 5 % CO_2 and 95% air and sub-cultured routinely using 0.02 % (w/v) EDTA trypsin (5 ml, 5min 37 °C, 5 % CO_2 incubation) once 100% confluence was reached.

Cytotoxicity assay. To ascertain the cytotoxic effect of all the compounds' treatment over a 24 h period, the 5-dimethylthiazol-2-yl-2,5 –diphenyltetrazolium bromide (MTT) assay was performed. Hela cells were trypsinized and plated to 70 % confluence in 96 well-plates 24 h before treatment. All compounds were then added at indicated concentrations to triplicate wells. Prior to the compounds' treatment, the DMEM was removed and replaced with fresh DMEM, and aliquots of the compounds stock solutions were diluted to obtain the final concentrations of 5, 10, 20, 40 and 80 μM. The treated cells were incubated for 24 h at 37 °C and under 5 % CO_2. Subsequently, the cells were treated with 5 mg/mL MTT (10 μL per well) and incubated for an additional 4 h (37 °C, 5 % CO_2). Then, DMEM was removed, the formazan crystals were dissolved in DMSO (100 μL per well), and the absorbance at 490 nm using a microplate reader (SpectraMax Paradigm).

Multicellulartumor spheroids formation. MCs formation In order to produce MCs, a layer of poly(2-hydroxyethyl methacrylate) (polyHEMA) thin film was coated on the bottom of tissue culture flasks. To ensure sterile, polyHEMA coated flask must be exposed to ultraviolet light for 2 h before use. HepG2 monolayer cells incubated as mentioned above were trypsinized to give a single-cell suspension and count the cell numbers using a hemocytometer. 5×10^5 cells in 5 mL of fresh DMEM medium was placed in a cell culture flask coated by polyHEMA. Cells were incubated at 37 °C in humidified atmosphere with 5% CO_2 and the culture medium was replaced every other day. HepG2 MCs (around 300 μm in diameter) formed spontaneously in 7 days.

Immunofluorescence. Prefixed brain slice was applied 0.5 %Triton X-100 for 5 min and washed by PBS 3 times for 5 min every time. After incubated with 100 mM glycine for 15 min at room temperature, PBS washed the slice again for 5min every time. Posteriorly, the slice was covered with 1 % BSA for 1 hour in order to close the non-specific binding sites for primary antibody, and incubated by using primary antibodies in the 4 degree refrigerator for more than 12 hours. After washing by PBS 3 times for 10 min every time, incubated with fluorescent second antibodies for 1 hour without exposure of light. The imaging was carried out after the slices washed by PBS for 3 times.

Confocal microscopic imaging. Confocal microscopy imaging was acquired with a Leica TCS SP8 confocal microscopy and ZEISS 880 two-photon confocal microscopy system, with 40X objective lens, 63X/100X oil-immersion objective lens. The incubated cells were excited at 405 nm for one-photon imaging, 633 nm for NucRed, 405 nm for DAPI, 488 nm for ER-tracker and fluorescent second antibody, 633 for NucRed. Two-photon confocal microscopy imaging of **MnFM1** and **MnFM2** were excited at 760 nm and the emission signals were detected in the region of 500-550 nm.

Confocal image processing and analysis. Micrographs were processing and analyzed by Huygens software and ImageJ 1.48 v (32-bit). Quantification of the fluorescence intensity was achieved via Analyze >> Tools >> ROI manager in ImageJ from three parallel experiments. Quantification of single cell intensity profile was achieved via Analyze >> Plot Profile by selecting one cell in ImageJ. Quantification of colocalizationcoefficency was achieve via an external plugin via Plugins >>Colocalization Finder. For more details, please refer to online sources: https://imagej.nih.gov/ij/.

Magnetic resistance imaging. Following the acquisition of a tripilot scan, T1-weighted MR images were acquired, typically along the coronal orientation, using a spin-echo sequence. For the mouse studies, the following acquisition parameters were chosen: repetition time (TR)=370 ms, echo time (TE)=11.6 ms, field of view (FOV)= 40 mm × 40 mm, matrix size= 192 × 192, slice thickness= 1 mm (12 slices, gap=0), 1 average, and bandwidth (BW)=50 kHz. For the rat studies, the following acquisition parameters were chosen: TR=590 ms, TE=13 ms, FOV=40 mm × 60 mm, matrix size=256 × 256, slice thickness=1 mm (30 slices, gap=0), 1 average, and bandwidth (BW)=50 kHz.

STED super resolution imaging. STED nasoscope experiments was performed under Leica DMi8 confocal microscopy equipped with Leica TCS SP8 STED-ONE unit and the compound was excited under STED laser, the emission signals were collected using HyD reflected light detectors (RLDs). Specimen living cells were prepared using similar method as normal confocal microscopy described previously, and donut laser used in 660nm STED laser (70% power), with 2048*2048 pixel and *100 scanning speed. The STED micrographs were further processed ‘deconvolution wizard’ function using Huygens Professional software (version: 16.05) under authorized license. The area radiuses were estimated under 0.02 micros with exclusion of 100 absolute background values. Maximum iterations were 40-time, signal-to-noise ration 20 was applied, with quality threshold 0.05; iteration mode: Optimized; Brick layout: Auto.

Tissue Section. Three-month-old male Kunming micewere terminally anaesthetised and transcardially perfused withphosphate buffered saline (PBS) 0.1 M pH=7.4. Their brains were extracted and the dura matercarefully removed.Brains from PBS-perfused animals were sectioned at 20 μM in the sagittal plane using a cryostat(Thermo Fisher Scientific, HM-560). Sections were mounted on glass slides, the nuclei stainedwith 4’,6-diamidino-2-phenylindole dilactate (DAPI; 300 nM in PBS; Sigma, D9564) for 1 min andcover-slipped using an aqueous Gold Anti-fade mountant (Thermo Fisher Scientific).

Animal experiment ethical statment: All procedures involving animals were approved by and conformed to the guidelines of the Southwest University Animal Care Committee, College of Pharmaceutical Sciences. We have taken great efforts to reduce the number of animal used in these

studies and also taken effort to reduce animal suffering from pain and discomfort.

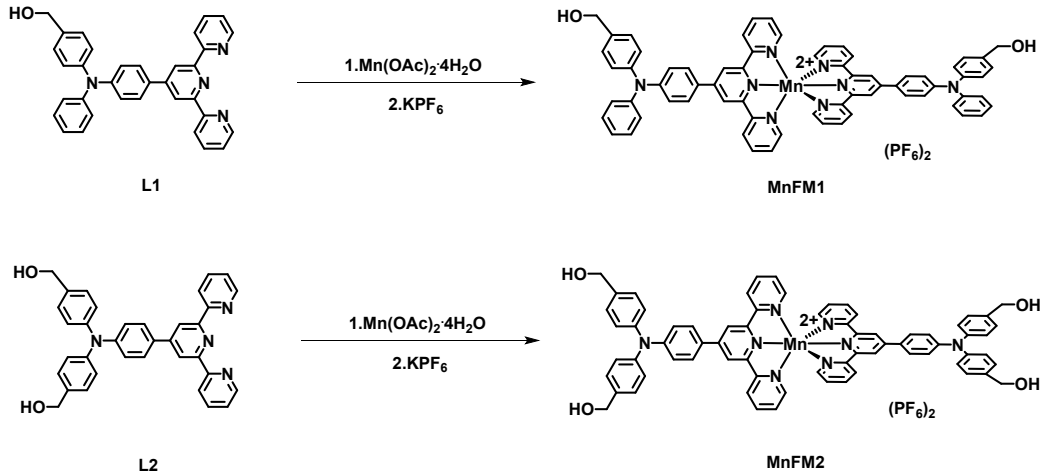

Scheme S1 Synthetic routes for **MnFM1** and **MnFM2**.

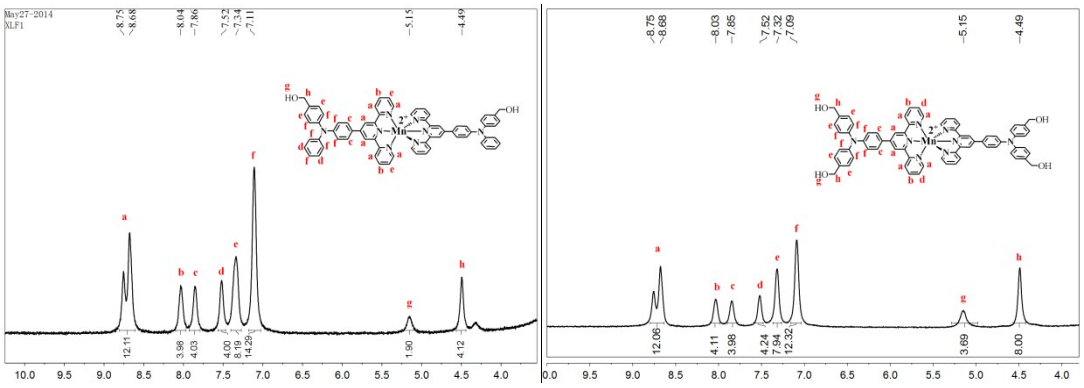

(a) (b)

Fig. S1 ^{1}H-NMR spectra of **MnFM1** (a) and **MnFM2** (b) in d_6-DMSO.

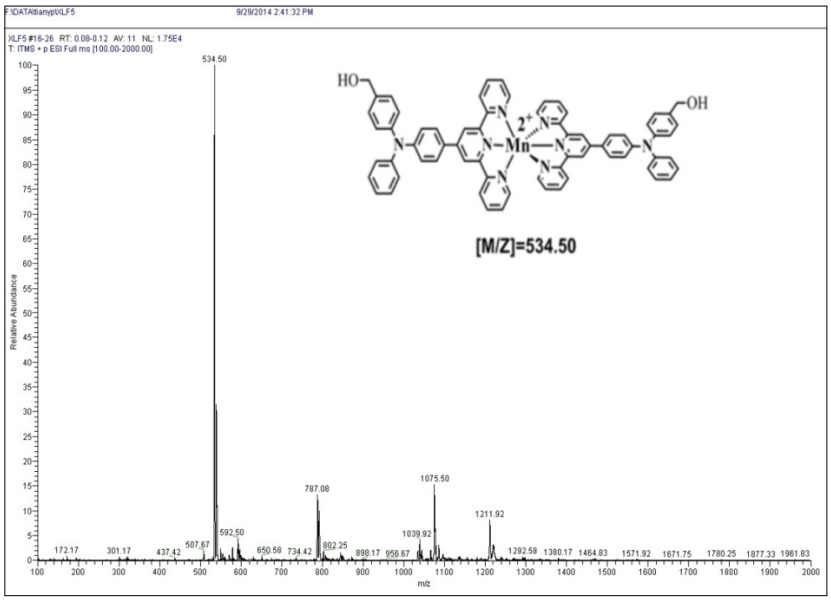

(a)

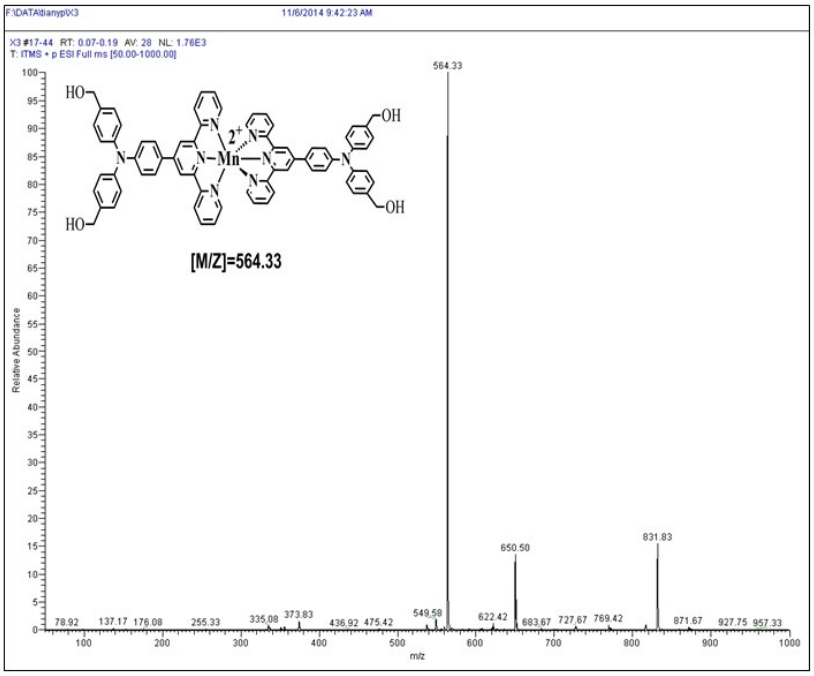

(b)

Fig. S2 ESI-MS spectra of **MnFM1** (a) and **MnFM2** (b).

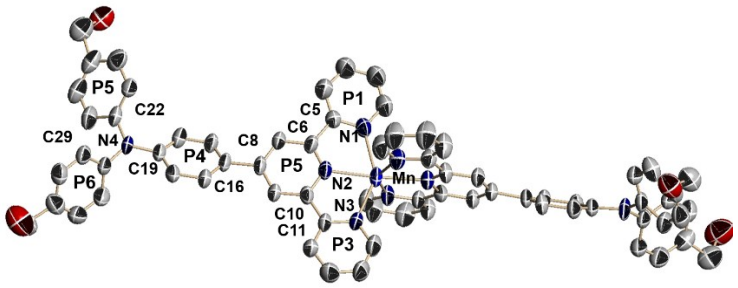

Fig. S3 The crystal structure of **MnFM2** (H atoms and PF_6^- anons are omitted for clarity, and disorder in the hydroxymethyl group).

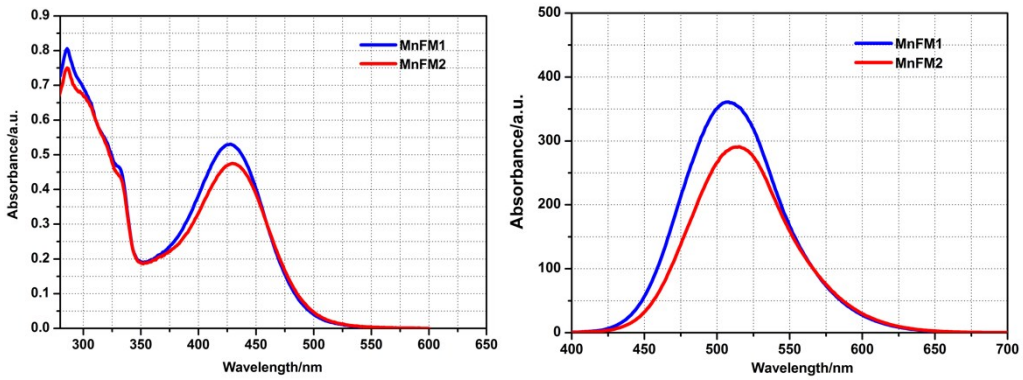

(a) (b)

Fig. S4 Linear absorption spectra (a) and single-photon fluorescence spectra (b) of **MnFM1** and **MnFM2** (in MeCN with c = 1×10^{-5} M).

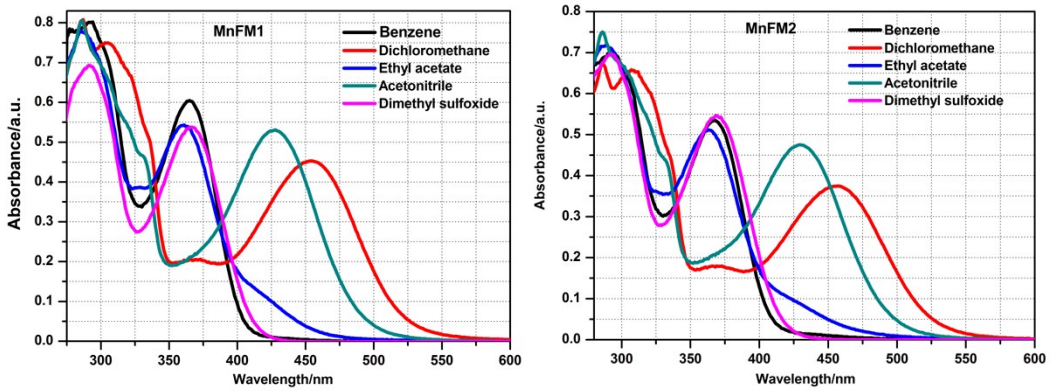

(a)

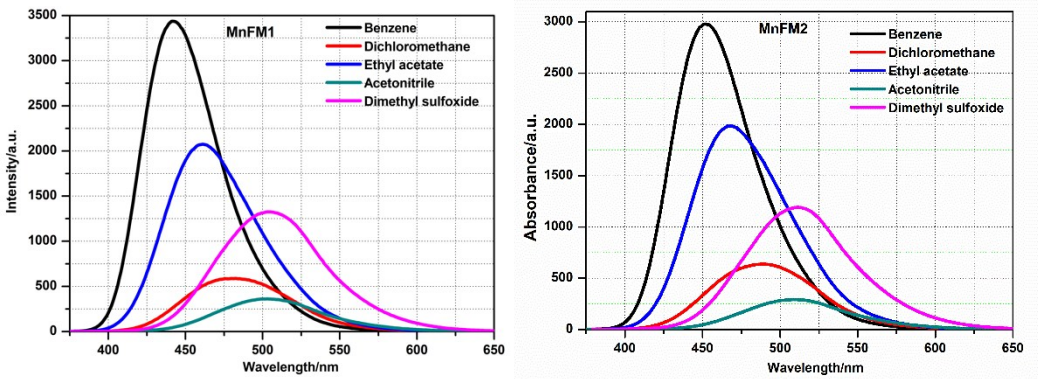

(b)

Fig. S5 Linear absorption (a) and single-photon excited fluorescence spectra (b) of **MnFM1** and **MnFM2** in five solvents with c=1.0×10^{-5} mol/L.

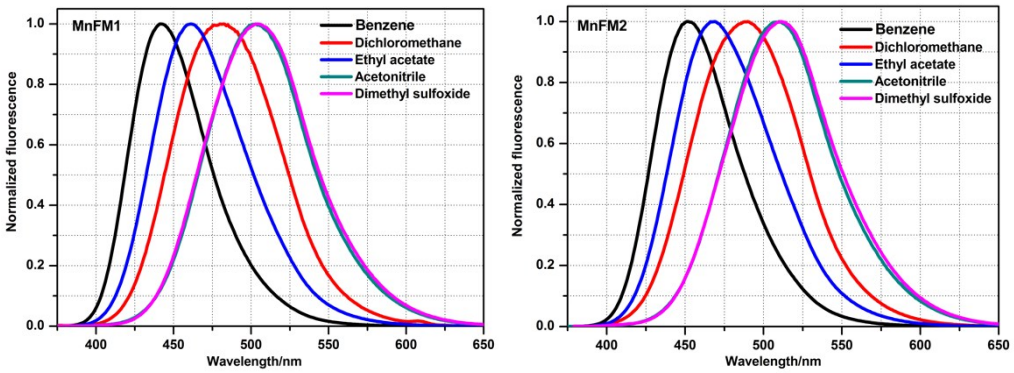

Fig. S6 Normalized fluorescence spectra of **MnFM1** and **MnFM2** in five solvents with c=1.0×10^{-5} mol/L.

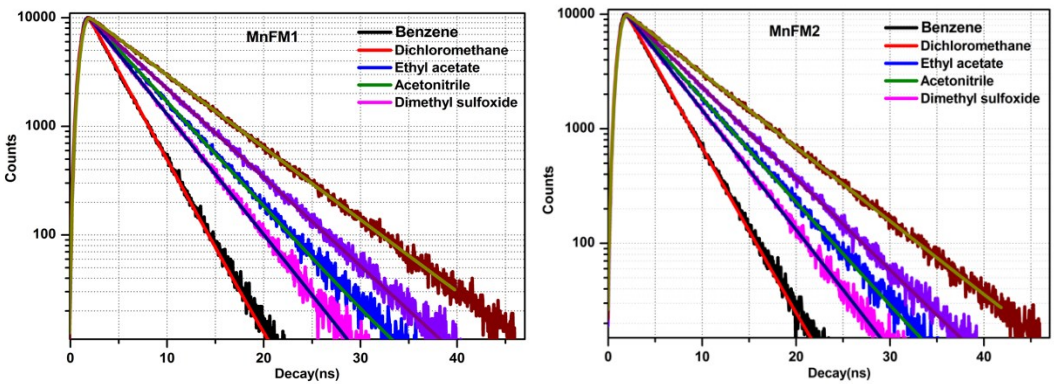

(a) (b)

Fig. S7 Time-resolved fluorescence curves of **MnFM1** and **MnFM2** in five solvents.

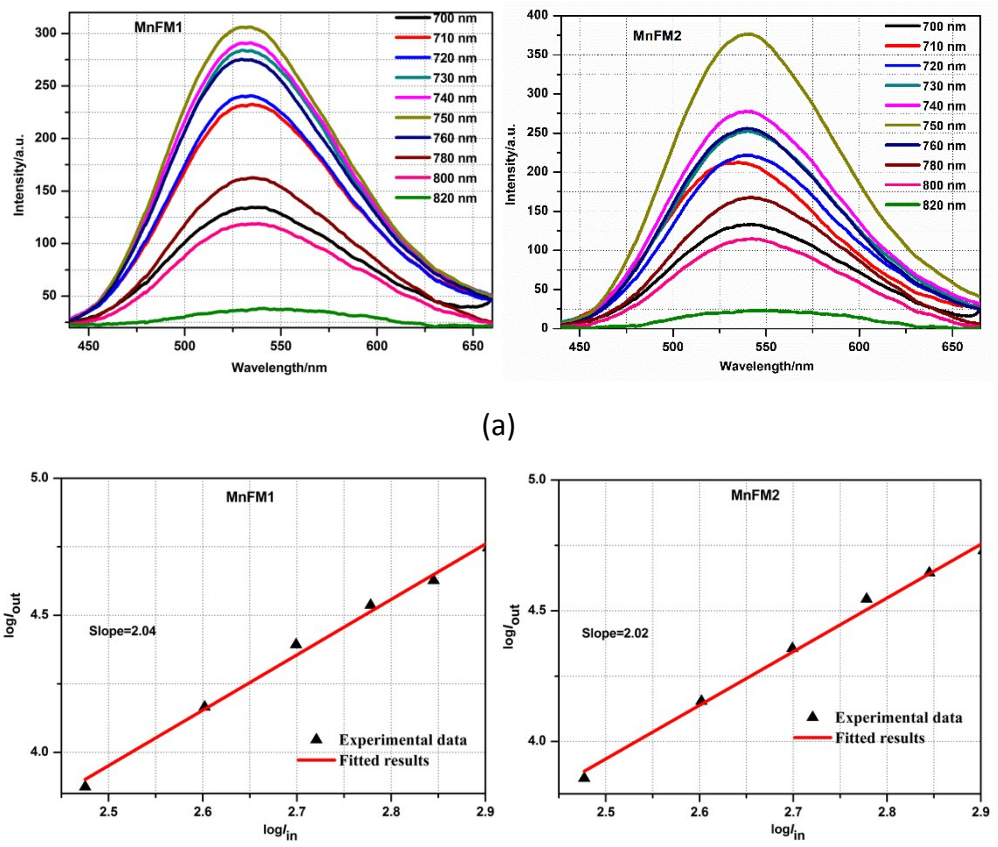

Fig. S8 (a) Two-photon fluorescence spectra of **MnFM1** and **MnFM2** in DMSO with c=1.0×10^{-3} mol/L by femtosecond laser pulses at 500 mW at different excitation wavelengths. (b) Output fluorescence (I_{out}) vs. the square of input laser power (I_{in}) of **MnFM1** and **MnFM2** excitation carried at 750 nm (c=1.0×10^{-3} mol/L, in DMSO).

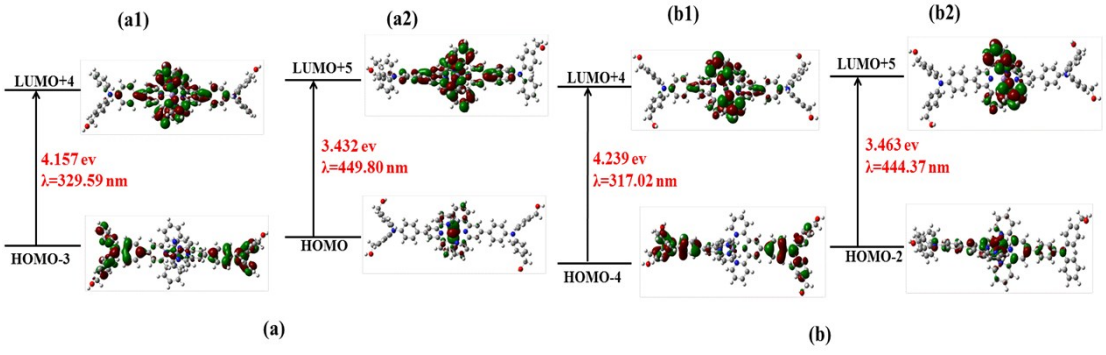

Fig. S9 Molecular orbital energy diagram for **MnFM1** (a) and **MnFM2** (b).

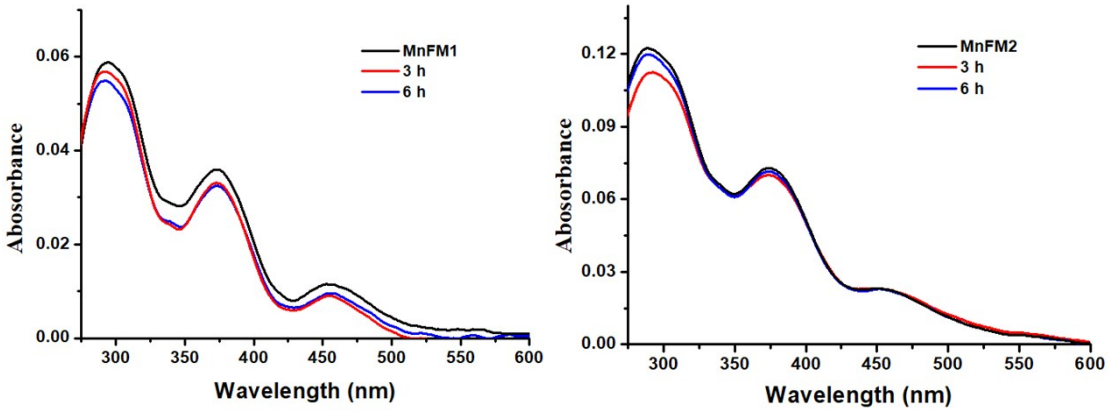

Fig. S10 Time evolution of UV-vis absorption spectra of **MnFM1** and **MnFM2** in PBS buffers.

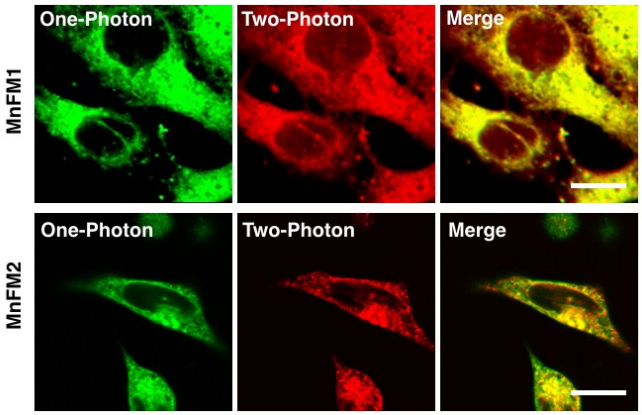

Fig. S11 Intracellular distribution assessment of 5 μM **MnFM1** and **MnFM2** on HepG2 cells over 30 minutes, under one-photon and two-photon confocal laser scanning microscopy, scale bar = 20 μm.

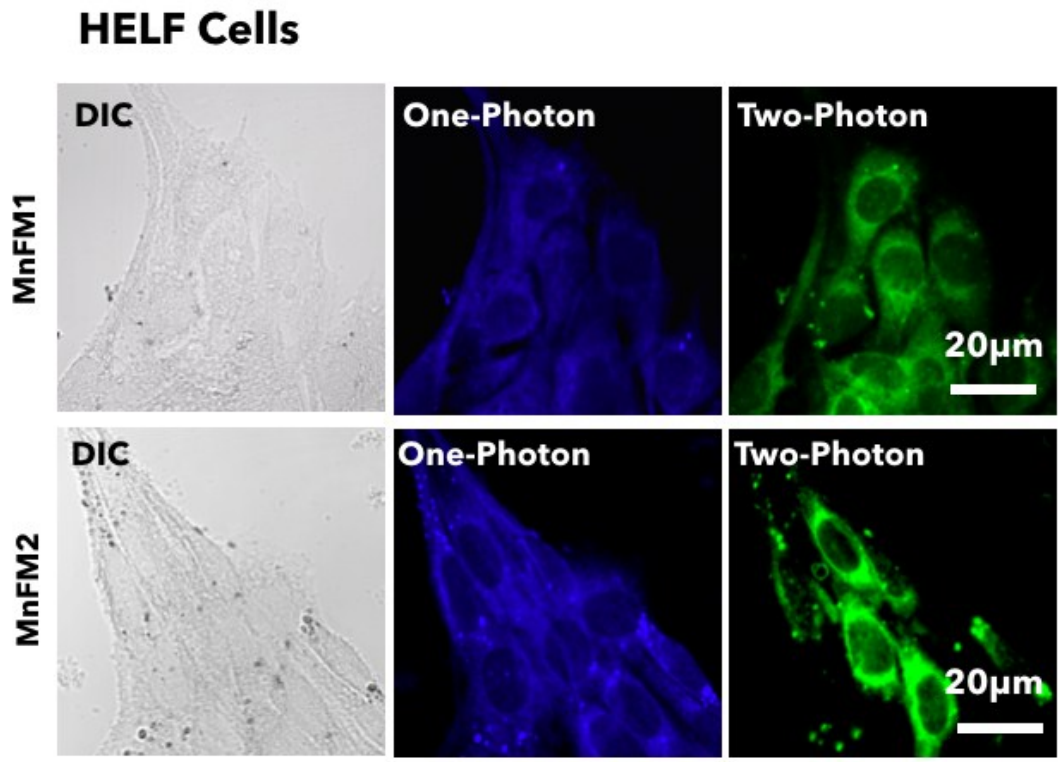

Fig. S12 Live cell uptake of **MnFM1** and **MnFM2** on human embryo liver fibroblast over 30 min.

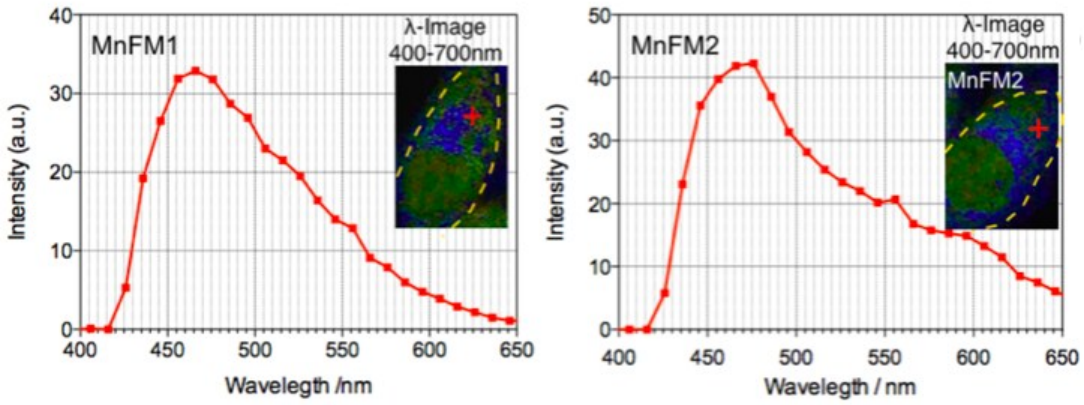

Fig. S13 λ-stacking scanning measure the emission intensity from 400-700nm from metal complexes internalized cells.

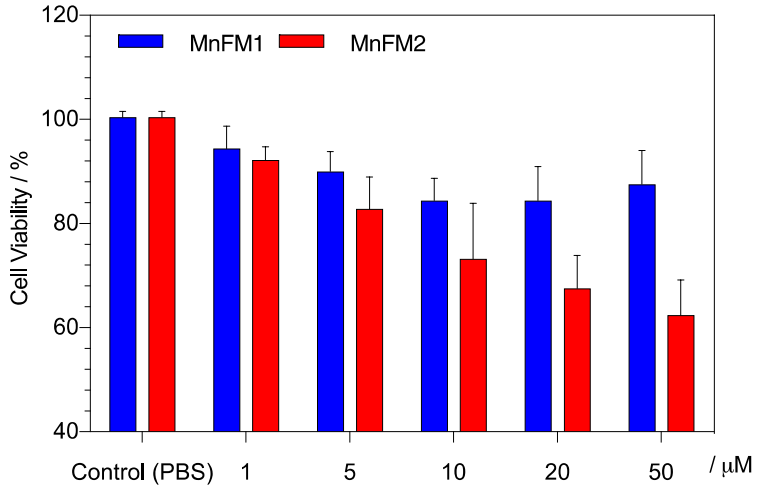

Fig. S14 MTT assay of different concentration of two metal complexes on HepG2 cells over 24 hours.

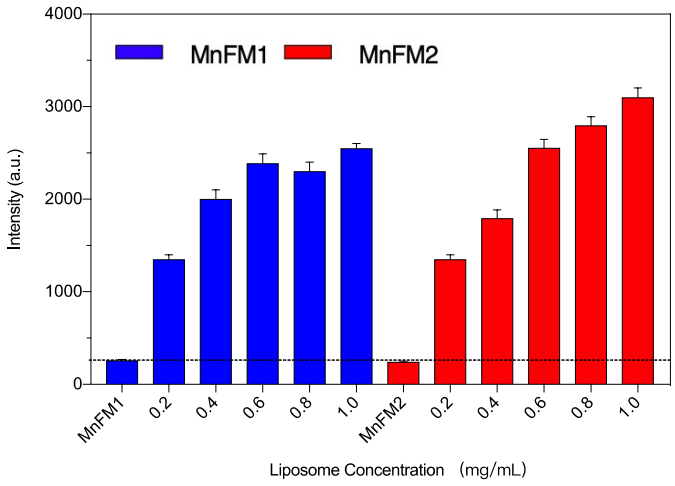

Fig. S15 Fluorescent intensity measurement using **MnFM1** and **MnFM2** (10 μM) with increasing concentrations of liposomes.

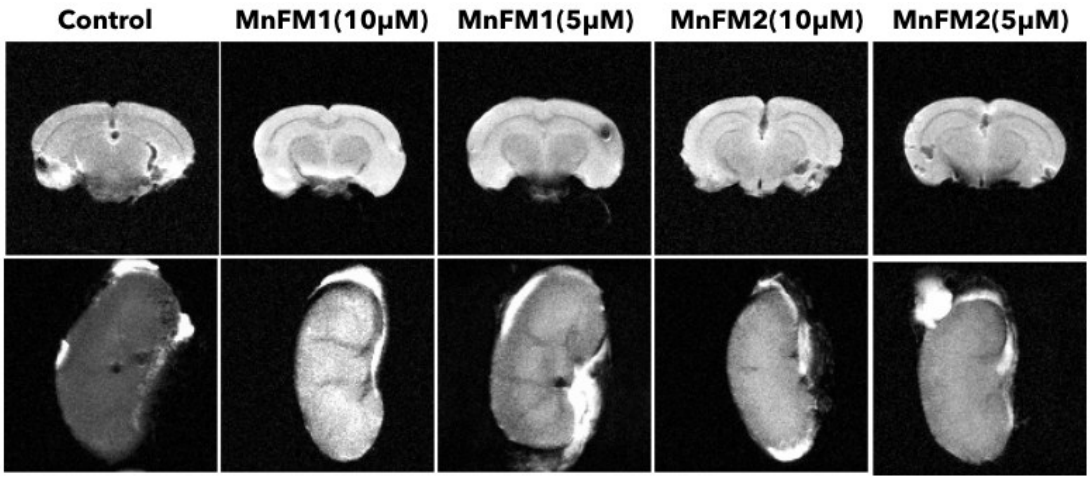

Fig. S16 Fixed mouse brain and kidney soaked into 5 and 10 μM **MnFM1** and **MnFM2**, respectively, imaged under nuclear magnetic resonance.

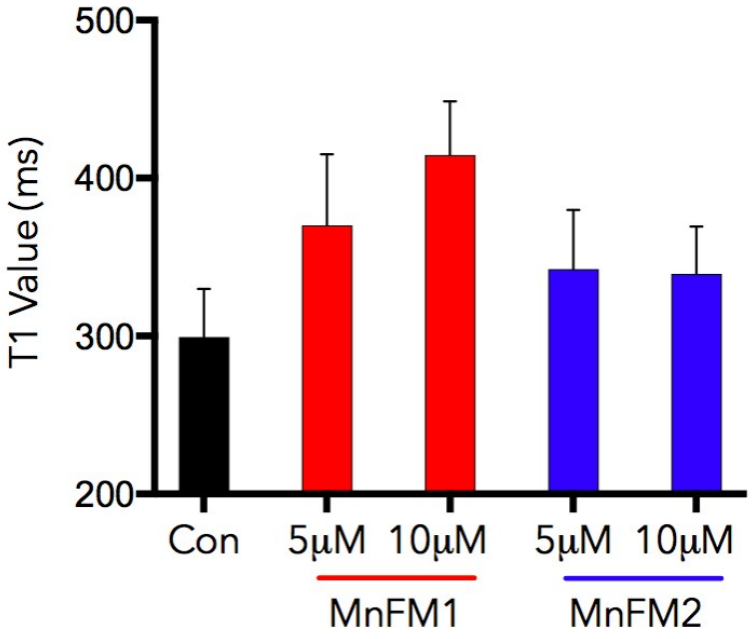

Fig. S17 T1 value of fixed mouse brain soaked into 10 μM **MnFM1** and **MnFM2**, imaged under nuclear magnetic resonance.

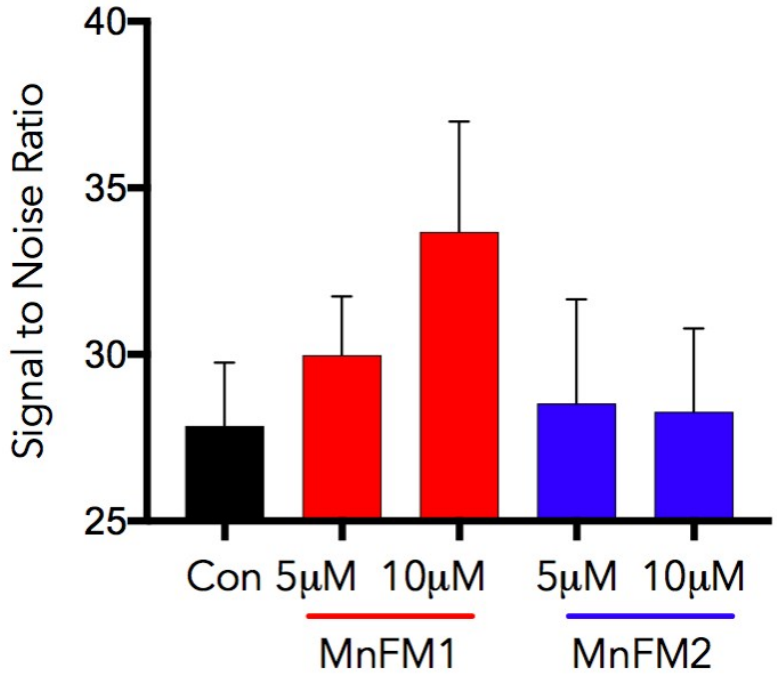

Fig. S18 MRI contrast analysis from **Fig. S16.**

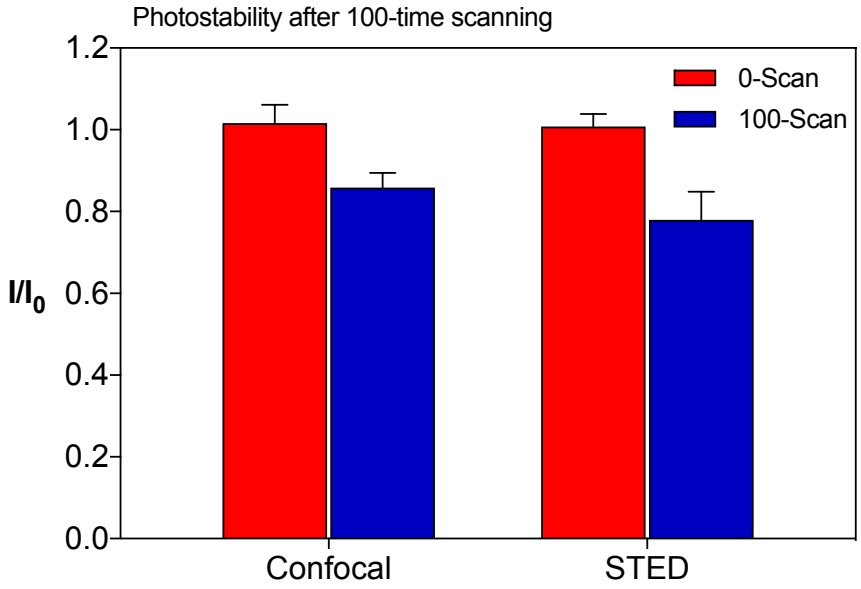

Fig. S19 Live cell photobleaching test using **MnFM1** under continued confocal (excitation wavelength = 405 nm, Emission = 500 nm) and STED (excitation wavelength = 405 nm, donuts laser = 595 nm) irradiation.

Table S1 Crystallographic data and structural refinement parameters of **MnFM2**.

Chemical formula	$C_{70}H_{60}F_{12}MnN_8O_6P_2$	***b*[º]**	96.400(4)
Formula weight	1454.14	***γ*[º]**	90.00
Crystal	Monoclinic	***V*(Å^3)**	3363.1(16)
Space group	P2/n	***Z***	2
***a*(Å)**	10.897(3)	R_1, wR_2 [$I \geq 2\sigma(I)$]	0.0697，0.2165
***b*(Å)**	10.372(3)	R_1, wR_2 [all data]	0.1662，0.2902
***c*(Å)**	29.943(8)	**S on F^2**	1.001
***α*[º]**	90.00	**CCDC**	1005127

Table S2 Selected bond lengths (Å) and angles (°) of **MnFM2**.

C8-C16	1.500(7)	C10-C11	1.472(7)	C5-C6	1.488(7)
C19-N4	1.395(6)	C22-N4	1.443(7)	C29-N4	1.420(7)
C19-N4-C22	121.5(4)	C22-N4-C29	115.9(4)	C19-N4-C29	122.6(4)
C1-N1-C5	117.4(5)	C6-N2-C10	119.1(4)	C11-N3-C15	117.0(5)
N1-Mn1	2.282(5)	N2-Mn1	2.193(4)	N3-Mn1	2.256(4)
N1-Mn1-N2	71.83(16)	N1-Mn1-N3	144.04(15)	N2-Mn1-N3	72.23(15)
N1-Mn1-N1A[a]	94.5(2)	N1-Mn1-N2A[a]	105.21(16)	N1-Mn1-N3A[a]	93.65(17)
N2-Mn1-N2A[a]	175.8(2)	N2-Mn1-N3A[a]	110.61(15)	N3-Mn1-N3A[a]	99.9(2)

[a] Symmetry transformations used to generate the equivalent atoms: -0.5-x, y, 1.5-z.

Table S3 Corresponding conformational parameters of **MnFM2.**

$P_{0,\ 4}$[a, b]	22.70°	$P_{1,\ 2}$	8.26°
$P_{0,\ 5}$	46.35°	$P_{2,\ 3}$	8.02°
$P_{0,\ 6}$	54.92°	$P_{2,\ 4}$	28.54°

[a] Representation of the dihedral angles between P_0 and P_4, and so on.

[b] The nitrogen of triphenylamine moiety and its three adjacent carbon atoms are approximately coplanar and name as the P_0 plane.

Table S4 Single-photon-related photophysical properties of **MnFM1** and **MnFM2** in five solvents.

Complexes	Solvents	λ_{max}[a](ε[b])	λ_{max}[c]	Φ[d]	τ(ns)[e]
MnFM1	C_6H_6	365(6.05)	441	0.48	2.67
	DCM	455(4.53)	480	0.29	4.51
	EtOAc	361(5.43)	461	0.32	3.92
	MeCN	428(5.31)	503	0.15	5.33
	DMSO	366(5.38)	504	0.28	6.52
MnFM2	C_6H_6	368(5.35)	452	0.50	2.98
	DCM	457(3.75)	490	0.36	4.79
	EtOAc	364(5.11)	469	0.34	4.17
	MeCN	430(4.75)	510	0.14	5.43
	DMSO	369(5.46)	511	0.25	6.72

[a] Peak position of the longest absorption band.

[b] Maximum molar absorbance in10^4 $mol^{-1}Lcm^{-1}$.

[c] Peak position of SPEF, exited at the absorption maximum.

[d] Quantum yields determined by using quinine sulfate as standard.

[e] The fitted fluorescence lifetime.

Table S5 Calculated linear absorption properties (nm), excitation energy (eV), oscillator strengths and major contribution for **MnFM1** and **MnFM2**.

Complexes	Experiment (λ, nm, MeCN)	Calculated (λ, nm)	E (eV)	Oscillator strengths (*f*)	Nature of the transitions	Characters
MnFM1	331	329.59	4.157	0.4875	HOMO-3→LUMO+4 (**Fig. S5 a1**)	ICT
	429	449.80	3.432	0.6232	HOMO→LUMO+5 (**Fig. S5 a2**)	MLCT
MnFM2	330	317.02	4.239	0.5088	HOMO-4→LUMO+4 (**Fig. S5 b1**)	ICT
	430	444.37	3.463	0.0533	HOMO-2→LUMO+5 (**Fig. S5 b2**)	MLCT

References

1. J. Liu, Q. Zhang, H. Ding, J. Zhang, J. Tan, C. Wang, J. Wu, S. Li, H. Zhou, J. Yang and Y. Tian, *Science China Chemistry*, 2013, **56**, 1315-1324.

2. L. Jie, W. hui, L. Dandan, Z. Hongping, T. Yupeng and W. Jieying, *Chinese Journal Structure Chemistry*, 2015, **34**, 365-372.